Oxidative Addition to Palladium(0) Made Easy through Photoexcited-State Metal Catalysis

Rajesh Kancherla[+], Krishnamoorthy Muralirajan[+], Bholanath Maity, Chen Zhu, Patricia Krach, Luigi Cavallo, and Magnus Rueping **

[*] Dr. R. Kancherla,[+] Dr. K. Muralirajan,[+] Dr. B. Maity, Prof. Dr. L. Cavallo, Prof. Dr. M. Rueping
KAUST Catalysis Center (KCC)
King Abdullah University of Science and Technology (KAUST)
Thuwal, 23955-6900 (Saudi Arabia)
E-mail: magnus.rueping@kaust.edu.sa

C. Zhu, P. Krach, Prof. Dr. M. Rueping
Institute of Organic Chemistry, RWTH Aachen University
Landoltweg 1, 52074 Aachen, (Germany)
E-mail: Magnus.Rueping@rwth-aachen.de

[+] These authors contributed equally

Abstract:. *Visible-light induced, palladium catalyzed alkylations of α,β-unsaturated acids with unactivated alkyl bromides are described. A variety of primary, secondary, and tertiary alkyl bromides are activated by the photoexcited palladium metal catalyst to provide a series of olefins at room temperature under mild reaction conditions. Mechanistic investigations and density functional theory (DFT) studies suggest that a photoinduced inner-sphere mechanism is operative in which a barrierless, single electron oxidative addition of the alkyl halide to Pd(0) is key for the efficient transformation*

Cross-coupling reactions are one of the most important synthesis tools for the formation of C–C or C–heteroatom bonds. Conventionally, three key steps are involved in the cross-coupling reaction: oxidative addition, transmetalation, and reductive elimination. Often challenges arise in the individual steps, depending on the coupling partners, metal catalysts or reaction conditions employed. In recent decades, numerous catalysts, as well as ligands, have been developed in order to reduce the energy barrier in the bond-forming and breaking steps. More recently, it has been shown that visible-light enhances cross-couplings employing radicals.[1] This methodology allows single electron transfer (SET) to replace the conventional two electron transfer process by using photoredox and transition metal dual-catalysis systems, thus significantly reducing the barrier for each step in cross-coupling reactions.[2] Despite developments made in cross-coupling chemistry, the conventional oxidative addition of alkyl electrophiles to Pd(0) remains sluggish, even at elevated temperature, due to the electron-rich nature of the alkyl halide bond.[3] In fact, computational studies have revealed that the alkyl bromide oxidative addition to Pd(0) is endothermic with a high energy barrier of 41.6 kcal/mol.

Further, alkyl-palladium(II) species that form *via* a two-electron transfer are considerably less stable due to the lack of π-electrons interacting with the empty d-orbitals of metal. This results in fast β-hydride (β–H) elimination from σ-alkyl-palladium(II) intermediates which outcompetes the required olefin insertion in decarboxylative alkylation cross-coupling reactions.[3, 4]

In contrast to the photoredox dual-catalysis strategy which promotes cross-coupling by lowering the energy barrier, we now report the use of a mechanistically distinct, SET barrierless oxidative addition strategy for alkylation of vinylic acids, using Pd complexes as both photosensitizer and cross-coupling catalyst.[5] This allows the oxidative addition barrier to be lowered resulting in an alkyl radical and Pd(I) intermediate (Figure 1) which can add to an α,β-unsaturated acids. Subsequent carbon dioxide elimination provides the akylated olefin and the regenerated catalyst. To the best of our knowledge, a visible light induced palladium catalyzed decarboxylative C(sp^3)–C(sp^2) cross coupling alkylation has not been reported.

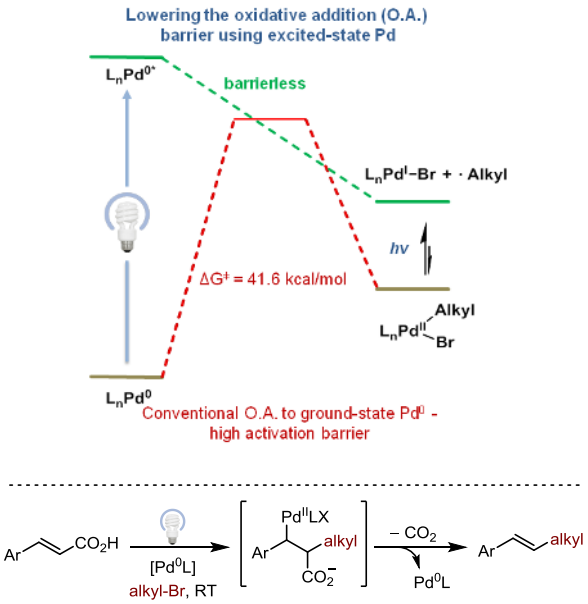

Figure 1. Visible-light assisted decarboxylative alkylation.

Vinylic acids are readily available and stable, which makes them versatile coupling partners in cross-coupling reactions forming C–C bonds.[6] As a result, decarboxylative reactions have been explored.[7] However, the use of pre-activated substrates, stoichiometric amounts of sacrificial reagents,[8] high temperature or the use of high energy UV irradiation may limit their synthetic applicability.[9] Therefore, the development of a cross-coupling alkylation of α,β-unsaturated acids with alkyl halides under mild reaction conditions, without the need for additional metal mediators or photocatalysts, would be a desirable goal.

With these considerations in mind, we started to examine a new visible light induced, palladium catalyzed alkylation by applying different catalysts and alkyl halides.[10] The reaction of cinnamic acid (**1a**) and cyclohexyl bromide (**2d**) in presence of $Pd(OAc)_2$, PPh_3 ligand and *N,N*-diisopropylethylamine (DIPEA) gave the (*E*)-substituted olefin **3d** in 82% yield with remarkable stereoselectivity of *E*/*Z* = 99:1 under irradiation with 34 W blue LEDs.[10] However, product formation was not observed when the reaction was carried out without light irradiation and at 100 °C. Among the other palladium sources examined, $Pd(PPh_3)_2Cl_2$ and $Pd(PPh_3)_4$ gave comparable yields of 87% and 76% respectively, whereas $PdCl_2$ was not reactive. PPh_3 was found to be a better ligand compared to Xantphos (11%) and PCy_3 (0%). Control experiments demonstrated that all components are necessary

to promote the reaction. Among a range of alkyl electrophiles tested, alkyl bromide was found to be more reactive (Br > I >> Cl) when compared to alkyl iodide (56%, due to possible side reactions) and alkyl chloride (< 1%, difficulty of oxidative addition).[10]

Using the optimized reaction conditions, the scope of the reaction was first evaluated with respect to the alkyl bromide (Table 1). A variety of tertiary, secondary, and primary alkyl bromides were found to react with excellent *E*-stereoselectivity, and a reactivity pattern of 3° ≥ 2° > 1° was observed. Especially, the reactivity and stereoselectivity of tertiary alkyl bromide with eliminable *β*-H is noteworthy (**3a** and **3b**).

Table 1. Reaction scope with respect to alkyl bromides.[a]

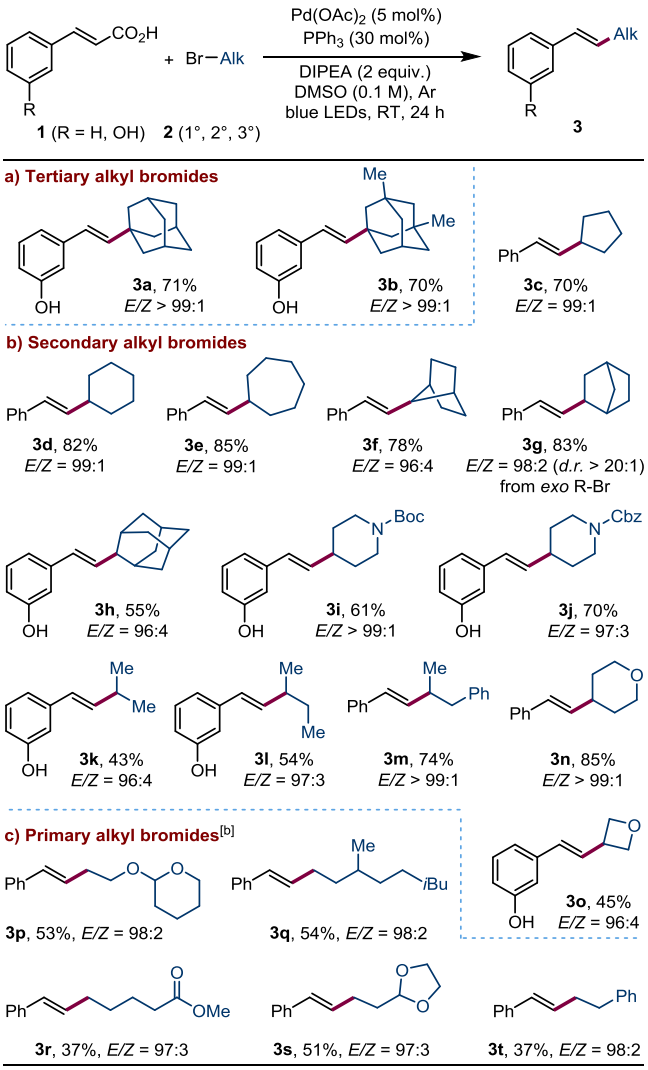

[a]Reaction conditions: **1** (0.2 mmol), **2** (0.3 mmol), 34 W blue LEDs, Ar, 24 h. Yields of isolated products. Ratio of stereoisomers was determined by ^{1}H NMR analysis. Temperature (T = 28 ± 2 °C). [b]$Pd(PPh_3)_4$ (10 mol%, 0.02 mmol) is used instead of $Pd(OAc)_2$ and PPh_3. See supporting information.

Secondary alkyl bromides with different chain lengths reacted with good selectivity and yields (**3c**-**3o**). A range of functional groups such as ether (**3n**-**3p**), ester (**3r**), acetal (**3s**), and amide (**3i** and **3j**) groups were well tolerated. Primary alkyl bromides could also be applied to give the olefinated products **3p**-**3t** with good stereoselectivity. Subsequently, the scope of the reaction with respect to substituted vinyl carboxylic acids was studied (Table 2).

Table 2. Reaction scope with respect to vinyl carboxylic acid.[a]

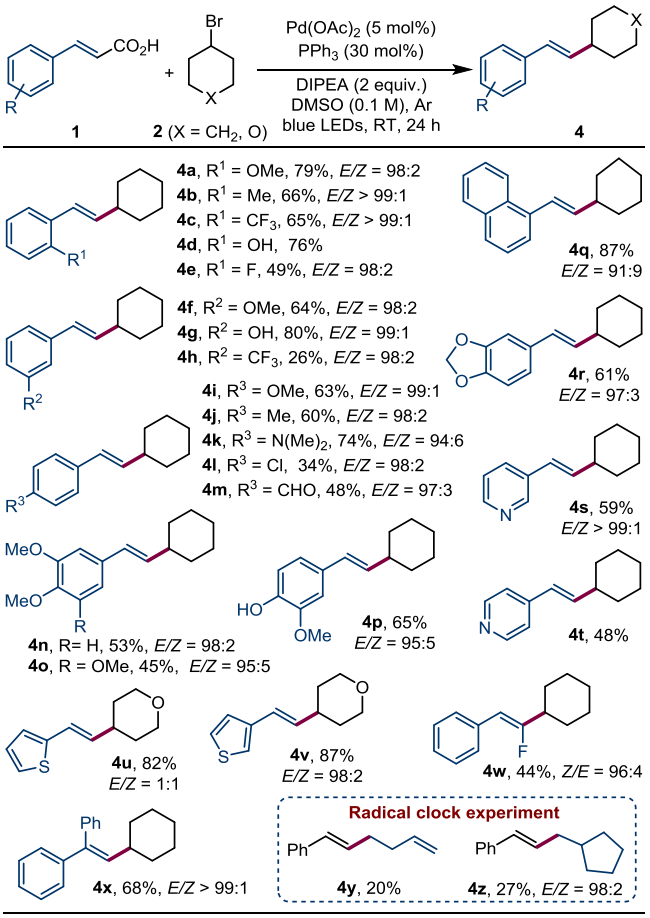

[a]Reaction conditions: **1** (0.2 mmol), **2** (0.3 mmol), 34 W blue LEDs, Ar, 24 h. Yields of isolated products. Ratio of stereoisomers was determined by ^{1}H NMR analysis. Temperature (T = 28 ± 2 °C). See supporting information.

Aryl and heteroaryl acrylic acids with both electron-rich and electron-deficient groups at *ortho*- (**4a**-**4e**), *meta*- (**4f**-**4h**), and *para*- (**4i**-**4m**) positions are amenable substrates. Additionally, a variety of functional groups including CF_3- (**4c** and **4h**), HO- (**4d**, **4g,** and **4p**), halide- (**4e** and **4l**), amino- (**4k**), aldehyde- (**4m**), and acetal groups (**4r**) were well tolerated. Typically, heterocyclic substrates with nitrogen and sulfur atoms can cause palladium poisoning due to the strong coordination of the heteroatom with a metal catalyst.[11] Notably, pyridinyl and thiophenyl acrylic acids showed good reactivity (**4s**-**4v**), even at room temperature. In addition to the 3-aryl acrylic acids, 3,3-diphenylacrylic acid is also an amenable substrate (**4x**). Reactions with *α*-substituted cinnamic acid or β-substituted styrenes to give (2,2-disubstituted vinyl)benzene are rare. However, under the optimized reaction conditions, α-fluorocinnamic acid was found to be reactive to give (*Z*)-(2-cyclohexyl-2-fluorovinyl)benzene (**4w**). In order to gain insight into the reaction mechanism radical clock and TEMPO trapping experiments were conducted to support the proposed light-mediated SET oxidative addition mechanism. Experiments with (bromomethyl)-cyclopropane and 6-bromohex-1-ene were performed which resulted in the formation of radical rearranged products **4y** and **4z** exclusively. TEMPO trapping experiments under standard conditions did not yield product **3d**; instead, a TEMPO-alkyl adduct was observed also supporting the radical mechanism.[10]

Further, to exclude the possibility of a radical chain process, light on-off experiments were carried out. During the light off-cycles no reaction was observed which confirms that light does not initiate a

chain-reaction.[10] The competition experiments between primary, secondary and tertiary alkyl bromides and the increased reactivity of secondary and tertiary alkyl bromides compared to primary alkyl bromides, clearly demonstrate that on photoirradiation, alkyl halides give thermodynamically more stable alkyl radicals that will undergo fast oxidative addition *via* a SET pathway rather than an S_N1 or S_N2 type oxidative addition.[4, 12]

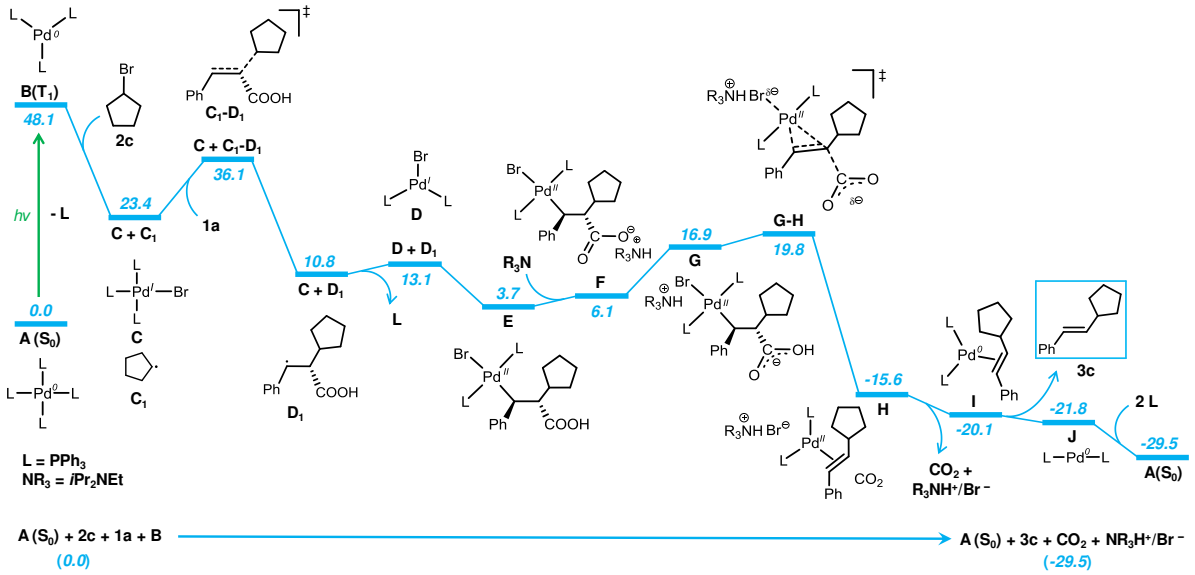

Figure 2. Computed energy profile for the decarboxylative alkylation of α,β-unsaturated acids. Free energies in solution (in kcal/mol) at the M06(SMD)/SDD/Def2-TZVP//PBE0/SDD/Def2-SVP level are displayed.

In the general context, it difficult to achieve the alkylation reaction since the majority of alkyl bromides possess lower reduction potentials ($E_{1/2}^{red} \geq$ -2.0 V vs. SCE) than *[$(Ph_3P)_4Pd$] ($E(M^+/M^*)$ = -1.72 V vs SCE in THF). Hence, we performed DFT calculations to unravel the mechanism of the newly developed decarboxylative alkylation of α,β-unsaturated acid (**1**) with cyclopentyl bromide (**2c**).[13] The *in-situ* generated $Pd^0(PPh_3)_4$ complex **A** is considered to be the reference structure for the calculations. Differently from the oxidative addition of aryl-halides within Mizoroki-Heck coupling,[14] the catalytically active $Pd^0(PPh_3)_2$ species **J** is reluctant to undergo oxidative addition of the alkyl-bromide **2c**, due to the very high energy barrier required to reach transition state **J-K** ($\Delta G^{\ddagger}$ = 41.6 kcal/mol, Figure S1). Having excluded the possibility of oxidative addition via a concerted 3−center reaction pathway, we explored a reaction pathway involving photoexcitation of Pd^0.[15,16] These calculations allowed us to identify the triplet state **B(T_1)** of $Pd^0(PPh_3)_3$, lying 48.1 kcal/mol higher than **A(S_0)**, as the active catalytic species (Figure S2, Table S1 for detail). The triplet **B(T_1)** furnishes an open coordination site for the bromoalkane **2c** association leading to an inner sphere photoinduced electron transfer (PET) with **2c**, a barrierless and exergonic step according to our computational protocol (Figure S3, Table S2), leading to the Pd^I-complex **C** with the liberation of cyclopentyl radical $\mathbf{C_1}$. Complex **C** is in equilibrium with the three-coordinated complex **D** via the slightly endergonic dissociation of a phosphine. Instead, radical $\mathbf{C_1}$ can attack cinnamic acid **1a** at the C_α atom via transition state $\mathbf{C_1}$-$\mathbf{D_1}$, with an activation free energy of 12.7 kcal/mol (Figures 2 and S4). The resulting $\mathbf{D_1}$ radical is 12.6 kcal/mol more stable than $\mathbf{C_1}$. At this point, the two doublet species **D** and $\mathbf{D_1}$ can collapse into the Pd^{II} intermediate **E**, with the release of 9.4 kcal/mol. Control calculations indicated that attack of $\mathbf{C_1}$ at the C_β atom of **1a** is unfavored by 2.1 kcal/mol (Figure S5).

Further progress in the reaction involves deprotonation of **E** by DIPEA, which leads to the zwitterionic complex **F**, lying 2.4 kcal/mol above **E** and prodromic to decarboxylation. The

decarboxylation step is facilitated by the endergonic rearrangement of DIPEA-H^+ from the side of the carboxylate group, near to the Br moiety, structure **G**. Although intermediate **G** is 10.8 kcal/mol less stable than intermediate **F**, proximity between DIPEA-H^+ and the Br atom helps the concerted elimination of CO_2 and of DIPEA-H^+/Br^- via transition state **G-H** (Figure S4), with a moderate energy barrier of 16.1 kcal/mol from intermediate **E**. In addition, forward evolution of transition state **G-H** leads to liberation of product **3c** and the $Pd^0(PPh_3)_2$ complex. Coordination of two phosphine to $Pd^0(PPh_3)_2$ regenerates **A(S_0)** for the next catalytic cycle, with a thermochemistry of the reaction **1a** + **2c** + DIPEA ⌫ **3c** + DIPEA-H^+/Br^- + CO_2 equal to -29.5 kcal/mol. Thus, the reaction can be considered to be composed of three fundamental steps (Figure 2): i) photoexcitation of a Pd^0 species to an active state promoting SET with the alkyl bromide to generate a Pd^I species and an alkyl radical; ii) addition of the alkyl radical to the α,β-unsaturated acid and coupling with the Pd^I species to generate a Pd^{II} species; iii) decarboxylation of the Pd^{II} species to liberate the product while regenerating the Pd^0 species.

Having clarified the reaction mechanism, we focused on the origin of the substantially barrierless SET between **B(T_1)** and **2c**.

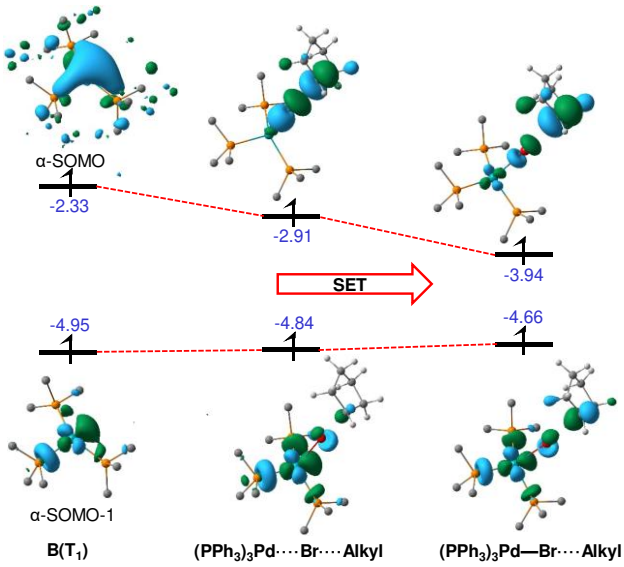

Figure 3. Molecular orbitals diagram showing the interaction between **B(T_1)** and **2c** during the SET step. Orbital energies are in eV. Phenyl groups are omitted for clarity.

The molecular orbitals diagram of Figure 3 shows that the SOMO of **B(T_1)** corresponds to a singly occupied MO mainly delocalized on the PPh_3 ligands with a minor Pd contribution, while the LUMO of **2c** corresponds to the σ* orbital of the Br–C bond. Analysis of an intermediate structure halfway along the PES connecting **B(T_1)** + **2c** to **C** + **C_1** indicates that during SET the SOMO of **B(T_1)** localizes on Pd and gets stabilized by mixing with the LUMO of **2c** (Figures 3 and S6), driving the reaction towards the formation of the Pd–Br bond and the rupture of the Br–C bond. The SOMO-1, which corresponds to a Pd centered MO (Figure 3), is not involved in the SET and its energy is marginally modified during the reaction. The energy difference $\Delta E^{\ddagger}$ between this intermediate structure and free reactants, the putative activation barrier, was decomposed into $\Delta E^{\ddagger} = \Delta E_{strain} + \Delta E_{int}$, where ΔE_{strain} is the energy required to deform the free reactants to the geometry they have in the intermediate structure, and ΔE_{int} is the interaction energy between the deformed reactants in the intermediate structure.[17] The calculated ΔE_{strain} and ΔE_{int} of 6.0 and -10.6 kcal/mol indicate that even at early stages of the reaction the interaction between the Pd SOMO and the Br–C bond σ* orbital is

strong enough to overcome the positive deformation energy and result in a negative (barrierless) $\Delta E^{\ddagger}$ of -4.6 kcal/mol.

In summary, by overcoming the challenges associated with the reactivity of ground-state palladium for the stereoselective decarboxylative alkylation of α,β-unsaturated acids, we discovered a low energy pathway using photo-excitation of palladium that allows a wide variety of primary, secondary, and tertiary alkyl halides to be applied in the decarboxylation reaction. In agreement with the experimental evidence, DFT calculations show that the oxidative addition of the alkyl-bromide to ground state Pd° is energy demanding. However, the PdL_3 species in its triplet state, generated by photoexcitation, can easily react with the alkyl-bromide via SET. The formed alkyl radical attacks the double bond of the *α,β*-unsaturated acid, leading to decarboxylation and product formation via a neutral pathway. In contrast to the outer sphere mechanisms observed in Ir and Ru based polypyridyl photocatalysts, the decarboxylative alkylation operates via a photoinduced inner sphere mechanism in which a barrierless, single electron oxidative addition of the alkyl halide to the metal is key for an efficient transformation.

Acknowledgements

P.E.K. thanks the Deutsche Bundesstiftung Umwelt for a doctoral stipend. The research leading to these results has received funding from the European Research Council under the European Union's Seventh Framework Programme (FP/2007-2013) / ERC Grant Agreement no. 617044 (SunCatChem).

Keywords: Palladium • Alkyl halide • Decarboxylation • Cinnamic acid • Excited-state • Barrierless • DFT

[1] Recent examples: a) J. Xie, J. Li, V. Weingand, M. Rudolph, A. S. K. Hashmi, *Chem. Eur. J.* **2016**, *22*, 12646-12650; b) X. Guo, O. S. Wenger, *Angew. Chem. Int. Ed.* **2018**, *57*, 2469-2473; c) C. B. Larsen, O. S. Wenger, *Chem. Eur. J.* **2018**, *24*, 2039-2058; d) J. Xie, H. Jin, A. S. K. Hashmi, *Chem. Soc. Rev.* **2017**, *46*, 5193-5203; e) F. Yang, J. Koeller, L. Ackermann, *Angew. Chem. Int. Ed.* **2016**, *55*, 4759-4762; f) N. Hoffmann, *Eur. J. Org. Chem.* **2017**, *2017*, 1982-1992; g) L. Li, X. Mu, W. Liu, Y. Wang, Z. Mi, C.-J. Li, *J. Am. Chem. Soc.* **2016**, *138*, 5809-5812; h) W. Liu, L. Li, C.-J. Li, *Nat. Commun.* **2015**, *6*, 6526; h) M. S. Oderinde, N. H. Jones, A. Juneau, M. Frenette, B. Aquila, S. Tentarelli, D. W. Robbins, J. W. Johannes, *Angew. Chem. Int. Ed.* **2016**, *55*, 13219-13223; i) M. S. Oderinde, M. Frenette, D. W. Robbins, B. Aquila, J. W. Johannes, *J. Am. Chem. Soc.* **2016**, *138*, 1760-1763.

[2] a) C. Le, T. Q. Chen, T. Liang, P. Zhang, D. W. C. MacMillan, Science **2018**, *360*, 1010-1014; b) J. C. Tellis, D. N. Primer, G. A. Molander, Science **2014**, *345*, 433-436; c) J. A. Terrett, J. D. Cuthbertson, V. W. Shurtleff, D. W. C. MacMillan, Nature **2015**, *524*, 330-334.

[3] a) A. C. Frisch, M. Beller, *Angew. Chem. Int. Ed.* **2005**, *44*, 674-688; b) N. Kambe, T. Iwasaki, J. Terao, *Chem. Soc. Rev.* **2011**, *40*, 4937-4947.

[4] S. Bräse, A. de Meijere, In *Metal-Catalyzed Cross-Coupling Reactions*; F. Diederich, P. J. Stang, Eds.; Wiley-VCH: Weinheim, 1998; Chapter 3.

[5] A. V. Kramer, J. A. Osborn, *J. Am. Chem. Soc.* **1974**, *96*, 7832-7833.

[6] Review on decarboxylation for C-C bond forming, see: T. Patra, D. Maiti, *Chem. Eur. J.* **2017**, *23*, 7382-7401.

[7] a) L. J. Goossen, G. Deng, L. M. Levy, *Science* **2006**, *313*, 662-664; b) Z. Wang, Q. Ding, X. He, J. Wu, *Org. Biomol. Chem.* **2009**, *7*, 863-865; c) K. Rousée, C. Schneider, S. Couve-Bonnaire, X. Pannecoucke, V. Levacher, C. Hoarau, *Chem. Eur. J.* **2014**, *20*, 15000-15004; d) G. Cahiez, A. Moyeux, M. Poizat, *Chem. Commun.* **2014**, *50*, 8982-8984; e) L. J. Goossen, N. Rodriguez, B. Melzer, C. Linder, G. Deng, L. M. Levy, *J. Am. Chem. Soc.* **2007**, *129*, 4824-4833.

[8] H. Huang, K. Jia, Y. Chen, *Angew. Chem. Int. Ed.* **2015**, *54*, 1881-1884.

[9] Examples of metal/peroxides reactions: for copper/peroxide: a) C.-Y. Wang, R.-J. Song, W.-T. Wei, J.-H. Fan, J.-H. Li, *Chem. Commun.* **2015**, *51*, 2361-2363; b) Z. Cui, X. Shang, X.-F. Shao, Z.-Q. Liu, *Chem. Sci.* **2012**, *3*, 2853-2858; c) H. Yang, P. Sun, Y. Zhu, H. Yan, L. Lu, X. Qu, T. Li, J. Mao, *Chem. Commun.* **2012**, *48*, 7847-7849; for iron/peroxide: d) H. Yang, H. Yan, P. Sun, Y. Zhu, L. Lu, D. Liu, G. Rong, J. Mao, *Green Chem.* **2013**, *15*, 976-981; for nickel and manganese/peroxide: e) J.-X. Zhang, Y.-J. Wang, W. Zhang, N.-X. Wang, C.-B. Bai, Y.-L. Xing, Y.-H. Li, J.-L. Wen, *Sci. Rep.* **2014**, *4*, 7446: example under UV irradiation: C. Wang, Y. Lei, M. Guo, Q. Shang, H. Liu, Z. Xu, R. Wang, *Org. Lett.* **2017**, *19*, 6412-6415.

[10] See the Supporting Information for details.

[11] Y.-J. Liu, H. Xu, W.-J. Kong, M. Shang, H.-X. Dai, J.-Q. Yu, *Nature* **2014**, *515*, 389.

[12] G. C. Fu, *ACS Cent. Sci.* **2017**, *3*, 692-700.

[13] Geometries were optimized with the PBE0 functional using the Def2-SVP basis set for non-metal atoms and the SDD-ECP basis set for Pd. Energies in solvent (DMSO) were calculated with the SMD solvation model at M06(SMD)/SDD(Pd)/Def2-TZVP(non-metals) method. Further details in the ESI.

[14] M. García-Melchor, A. A. C. Braga, A. Lledos, G. Ujaque, F. Maseras, *Acc. Chem. Res.* **2013**, *46*, 2626-2634.

[15] a) D. Kurandina, M. Parasram, V. Gevorgyan, *Angew. Chem. Int. Ed.* **2017**, *56*, 14212-14216; b) G.-Z. Wang, R. Shang, W.-M. Cheng, Y. Fu, *J. Am. Chem. Soc.* **2017**, *139*, 18307-18312; c) D. Kurandina, M. Rivas, M. Radzhabov, V. Gevorgyan, *Org. Lett.* **2018**, *20*, 357-360; d) M. Koy, F. Sandfort, A. Tlahuext-Aca, L. Quach, C. G. Daniliuc, F. Glorius, *Chem. Eur. J.* **2018**, *24*, 4552-4555; e) G.-Z. Wang, R. Shang, Y. Fu, *Org. Lett.* **2018**, *20*, 888-891.

[16] For other reports on photochemically induced SET from Pd(0), see: a) P. Chuentragool, M. Parasram, Y. Shi, V. Gevorgyan, *J. Am. Chem. Soc.* **2018**, *140*, 2465-2468; b) R. Maxim, P. Marvin, W. Yang, V. Gevorgyan, *Angew. Chem. Int. Ed.* **2018**, *57*, 2712-2715; c) W.-J. Zhou, G.-M. Cao, G. Shen, X.-Y. Zhu, Y.-Y. Gui, J.-H. Ye, L. Sun, L.-L. Liao, J. Li, D.-G. Yu, *Angew. Chem. Int. Ed.* **2017**, *56*, 15683-15687; d) M. Parasram, P. Chuentragool, Y. Wang, Y. Shi, V. Gevorgyan, *J. Am. Chem. Soc.* **2017**, *139*, 14857-14860.

[17] a) L. Falivene, S. M. Kozlov, L. Cavallo, *ACS Catal.* **2018**, *8*, 5637-5656. b) W.J. van Zeist, F. M. Bickelhaupt, *Org. Biomol. Chem.* **2010**, *8*, 3118-3127.